Available online at www.sciencedirect.com

SCIENCE DIRECT®

International Journal of Thermal Sciences 45 (2006) 955–961

International Journal of Thermal Sciences

www.elsevier.com/locate/ijts

Thermal performance of silicon micro heat-sinks with electrokinetically-driven flows ☆

Gian Luca Morini [a,*], Marco Lorenzini [a], Sandro Salvigni [a], Marco Spiga [b]

[a] *DIENCA, Università degli Studi di Bologna, Viale Risorgimento 2, I-40136 Bologna, Italy*
[b] *Dipartimento di Ingegneria Industriale, Parco Area delle Scienze 181A, I-43100 Parma, Italy*

Received 10 September 2005; accepted 16 January 2006

Available online 28 February 2006

Abstract

A heat sink consisting of microchannels of rectangular or trapezoidal cross-section through which a polar fluid is circulated by means of an electro-osmotic pump was studied numerically. The equivalent pressure head—volume flow rate curve was determined for both geometries and the influence of the aspect ratio was investigated. The dimensionless temperature profile was calculated taking also the effect of Joule heating into account. The cross-sectional Nusselt number was determined for the above conditions and was found to be strongly influenced by the ratio of Joule heating to convective heat flux, M_z. The dependence of the Nusselt number on the dimensionless electro-osmotic diameter (kD_h) was also investigated for the two geometries and for increasing values of M_z, and a comparison with the values obtained analytically for slug flow under the same conditions was made. The value of the Nusselt number, as a function of the aspect ratio, was also calculated for increasing values of M_z. The numerical data presented in this paper can be useful to optimize silicon micro heat-sinks in terms of thermal performance.

Keywords: Microchannel; Electric double layer (EDL); Joule heating; Electro-osmotic pumps; Electronic cooling; Nusselt number

1. Introduction

Heat and fluid flow within microchannels has been the subject of much interest in the past decade, owing also to the ever-increasing progress in microfabrication techniques, which has steadily broadened the number of applications which exploit the high heat removal rate of laminar flow in micro-conduits. Convective flows within microchannels are usually driven by an imposed pressure gradient; however, this kind of technique becomes inadequate or very demanding in terms of pressure head when the hydraulic diameter drops below 100 μm. Conventional micro-pumps manufactured up to now showed limitations in terms of efficiency and reliability, which led to the investigation of alternative methods to circulate the fluid. One of these consists of "dragging" the fluid using an externally applied electric field by means of the electro-osmotic effect, which has been fundamentally understood for about two centuries (Reuss [1]). The flow thus generated is called electro-osmotic flow (EOF) and is of practical importance in microchannels, where the thickness of the electric double layer can become of the same order of magnitude as the characteristic dimensions of the channel, as detailed below.

The effect of electro-osmotic coupling between fluid and walls in pressure-driven flows has been investigated analytically by Mala et al. [2,3], Yang and Li [4], Yang et al. [5] and Li [6]: these papers deal with the solution of the Navier–Stokes equations in the case of internal flows with electrostatic forces through microchannels with rectangular cross section or parallel plate configuration. One aspect which has been evidenced in these works is the influence on the friction factor of electrostatic interaction between fluid and channel walls [2–6] and on the Nusselt number [3,5]. In particular, an increase of the friction factor with the ionic concentration in the liquid and a dependence of the Nusselt number on the Reynolds number, even in the fully developed laminar regime,

☆ A preliminary version of this paper was presented at ICMM05: Third International Conference on Microchannels and Minichannels, held at University of Toronto, June 13–15, 2005, organized by S.G. Kandlikar and M. Kawaji, CD-ROM Proceedings, ISBN: 0-7918-3758-0, ASME, New York.

* Corresponding author. Tel.: +39 051 2093287; fax: +39 051 2093296.
E-mail address: gianluca.morini@mail.ing.unibo.it (G.L. Morini).

1290-0729/$ – see front matter
doi:10.1016/j.ijthermalsci.2006.01.009

Nomenclature

e	electron charge	C
g	coefficient used in Eq. (9)	
k	Debye–Huckel parameter	m^{-1}
n_0	average ion concentration	M
p	pressure	Pa
q'	specific heat flux	$\mathrm{W\,m^{-1}}$
u	velocity	$\mathrm{m\,s^{-1}}$
u^*	dimensionless velocity, $= u/U$	
z	ion valence	
C	contour of the microchannel	m
C^*	dimensionless contour, $= C/D_h$	
D_h	hydraulic diameter	m
E_z	electric potential at the electrodes	$\mathrm{kV\,m^{-1}}$
E_z^*	dimensionless electric potential, $= \frac{E_z L}{\zeta}$	
H	height of the microchannel	m
L	length of the microchannel	m
L^*	dimensionless length of the microchannel, $= L/D_h$	
M_z	dimensionless Joule heating	
Nu	Nusselt number	
Po	Poiseuille number	
Q_{th}	thermal power removed	W
Q_v	volumetric flow rate	$\mathrm{\mu l\,min^{-1}}$
S	microchannel cross-sectional area	m^2
S^*	dimensionless surface, $= S/D_h^2$	
T	temperature	K
T^*	dimensionless temperature, $= \lambda \frac{(T-T_w)}{q'}$	
T_w	wall temperature	K
U_m	average velocity	$\mathrm{m\,s^{-1}}$
U	reference velocity	$\mathrm{m\,s^{-1}}$
W	half-width of the microchannel	m

Greek symbols

β	aspect ratio	
ε_0	electric permittivity of vacuum	$\mathrm{CV^{-1}\,m^{-1}}$
ε_r	relative electric permittivity	
κ_b	Boltzmann's constant	$\mathrm{J\,K^{-1}}$
ζ	zeta potential	V
ζ^*	dimensionless zeta potential, $= \frac{ze}{\kappa_b T}\zeta$	
μ	dynamic viscosity	Pa s
λ	thermal conductivity	$\mathrm{W\,m^{-1}\,K^{-1}}$
λ_0	electrical conductivity	$\mathrm{\Omega^{-1}\,m^{-1}}$
Ψ	electrical potential	V
Ψ^*	dimensionless electrical potential, $= \frac{ze}{\kappa_b T}\Psi$	

Subscripts and superscripts

$*$	non-dimensional quantity
0	electrical
m	average
r	relative
sf	slug flow
th	thermal
v	volumetric
w	wall

have been predicted. Santiago [7] analysed the dynamic behaviour of a liquid driven by electro-osmotic forces in a channel bounded by parallel plates. Maynes and Webb conducted an analytical investigation on the convective heat transfer in micropipes subject to constant heat flux or constant wall temperature [8,9].

Tang et al. [10] investigated the importance of Joule heating in liquid EOF. It was pointed out that the dependence of temperature on the ionic diffusion coefficients and Joule heating can greatly influence the velocity profile and heat transfer within a microchannel.

Arulanandam and Li [11] executed a numerical study to characterise the EOF: their model allows investigation of the dependence of the volume flow rate on the microchannel's geometrical characteristics, on ion concentration in the fluid and on the electric potential at the electrodes.

In the present work, the model of Arulanandam and Li [11] is utilized in order to investigate the dynamical and thermal performance of silicon microchannels with rectangular or trapezoidal cross-sections through which a liquid EOF is circulated. The microchannel geometries considered in this paper are those typical for silicon micro heat-sinks; in fact, the microchannels obtained by chemical etching on silicon wafers have usually a rectangular (silicon ⟨110⟩) or trapezoidal with a base angle of 54.74° (silicon ⟨100⟩) cross section.

The effects of Joule heating within the flowing medium on the convective heat transfer coefficients will be considered in the analysis. Simulation of the electro-osmotic flow can give the design engineer detailed information on matters such as electrical potential distribution along the microchannel, velocity distribution at the generic cross-section, relation between the electrical potential at the electrodes and the circulated flow rate, temperature distribution and values of the Nusselt number. The results have been obtained numerically by solving the model's equations with the finite element method (FEM) and validating the data by comparing them with those obtained by Arulanandam and Li [11] under the same conditions.

2. Analysis of the electro-osmotic flow

A solid surface becomes loaded with electrical charges when it is brought into contact with an electrolyte (polar liquid). In the case of glass and silica, the deprotonation of surface silanol groups (SiOH) is responsible of the generated surface charge density. In response to the generated surface charge, nearby ions of opposite charge in the electrolyte are attracted to the liquid-solid interface. A region near the surface in which a net excess of mobile ions with a polarity opposite to that of the walls is thus created: this region is called *electric double layer* (EDL). The EDL can be divided into two regions: the *compact layer*, the sub-region closer to the wall, characterised by high values of the electrical potential and the *diffuse layer*, where the gradient in ionic concentration gradually decreases. The plane separating the two layers is called *Stern plane* or *shear plane*. For fluids with low ionic concentration, the thickness of the EDL can reach several hundreds of nanometers (e.g. about 1 μm for deionised, ultra-filtered water, DIUF), and thus become comparable in size with the typical dimensions of the microchannel employed in micro heat-sinks.

If a pressure-driven flow is imposed through the microchannel, the ions in the mobile part of the EDL are carried towards one end. This causes an electrical current (*streaming current*) to flow in the direction of the liquid flow. The accumulation of ions downstream sets up the streaming potential that it is responsible for the *conduction current* which flows back in the opposite direction. Under equilibrium conditions, the conduction current equals the streaming current and a steady-state is reached. When an electric field is applied along the microchannel—e.g. by means of two electrodes—tangentially to the EDL, the diffuse layer of the EDL is drawn towards the negative electrode and this results in a convective flow in the same direction: the electro-osmotic flow (EOF).

In this paper a silicon micro heat-sink with trapezoidal or rectangular channels through which a laminar, steady and fully developed electro-osmotic flow (EOF) of a polar fluid is subjected to an uniform heat flux (H1 thermal boundary condition) will be analysed. No external pressure difference between the inlet and outlet of the microchannels is imposed.

The mathematical model of EOF developed in this study starts from the Poisson–Boltzmann equation governing the electrical potential distribution that, in dimensionless form, can be written as follows (see, e.g. [11]):

$$\nabla^{2*}\Psi^* = (kD_h)^2 \sinh(\Psi^*) \tag{1}$$

where the asterisk denotes the fact that quantities are non-dimensional and the Debye–Huckel parameter appears:

$$k = \left(\frac{2n_0 z^2 e^2}{\varepsilon_r \varepsilon_0 \kappa_b T}\right)^{1/2} \tag{2}$$

The inverse of this parameter $(1/k)$, called the Debye length, gives the magnitude of the diffuse layer thickness. It can be demonstrated that the value of the dimensionless electrokinetic potential for a given cross-section is strongly dependent on the product kD_h sometimes called the dimensionless electro-osmotic diameter. The boundary condition associated to Eq. (1) is the following:

$$\Psi^*|_{C^*} = \zeta^* \tag{3}$$

where ζ^* is the value of the dimensionless electrokinetic potential on the Stern plane, the so-called *zeta potential*.

The modified Navier–Stokes equations are used to describe the motion of an electrolyte driven by electrokinetic body forces related to the electrical potential distribution in the fluid [11]:

$$\nabla^{2*}u^* = E_z^* \sinh(\Psi^*) \tag{4}$$

with the non-slip boundary condition at the channel walls:

$$u^*|_{C^*} = 0 \tag{5}$$

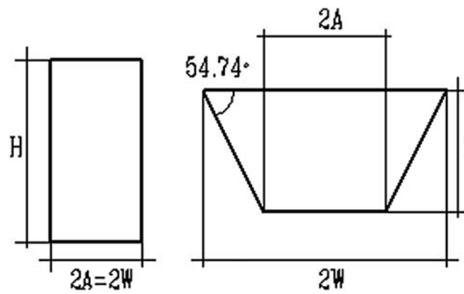

Fig. 1. KOH-etched microchannel cross-sections: rectangular and trapezoidal.

The dimensionless velocity u^* involved in Eq. (4) is defined by using the following reference velocity:

$$U = \frac{2nze\zeta D_h^2}{\mu L} \tag{6}$$

The velocity distribution allows the immediate calculation of the volumetric flow rate:

$$Q_v = U D_h^2 \int_{S^*} u^* \, \mathrm{d}S^* = U_m S^* D_h^2 \tag{7}$$

where S^* is the non-dimensional cross-section ($S^* = S/D_h^2$) and U_m is the mean fluid velocity in the microchannel. Finally, the equivalent pressure head for an electro-osmotic flow can be calculated from the following equation:

$$\left.\frac{\mathrm{d}p}{\mathrm{d}z}\right|_{\mathrm{eq}} = \frac{\mu Po_g(\beta) Q_v}{2S^* D_h^4} \tag{8}$$

in which $Po_g(\beta)$ is the Poiseuille number (defined as the product between the Darcy–Weisback friction factor and the Reynolds number).

The Poiseuille number depends on the geometry of the cross section; the aspect ratio β of the microchannel is defined as the ratio between the height (H) and the maximum width $(2W)$ of the section (see Fig. 1). For rectangular and trapezoidal microchannels the Poiseuille number can be calculated as a function of the channel aspect ratio ($\beta = H/2W$) by means of the following correlation proposed by Morini [12]:

$$Po_g(\beta) = 4\sum_{n=0}^{5} g_i \beta^n \tag{9}$$

where the g_i denote constant coefficients obtained through a least-squares best fit of the numerical data. A similar correlation has been presented by Shah and London [13] for rectangular ducts.

The values of the constants g_i are listed in Table 1 for microchannels having rectangular and trapezoidal cross sections; the maximum relative difference Δ reported in Table 1 is positive when Eq. (9) gives values greater than the rigorous calculation.

The parameter defined by Eq. (8) corresponds to the equivalent pressure gradient which would ensure the same flow rate if a pressure-driven flow were considered in the same microchannel.

Eqs. (1) and (4) with their boundary conditions were numerically solved for the cross-sectional geometries of interest by

Table 1
Weighing coefficients for the calculation of the Poiseuille number by means of Eq. (9)

Trapezoidal ⟨100⟩ silicon microchannel (Morini [12]) $0 < \beta < 0.707$						
g_0	g_1	g_2	g_3	g_4	g_5	Δ(%)
24	−42.267	64.272	−118.42	242.12	−178.79	−0.14
Rectangular ⟨110⟩ silicon microchannel (Shah and London [13]) $0 < \beta < 1$						
g_0	g_1	g_2	g_3	g_4	g_5	Δ(%)
24	−32.5272	46.7208	−40.8288	22.9536	−6.0888	0.05

Table 2
Operating conditions for the EOF analyzed by Arulanandam and Li [11]

β	n_0 [M]	ε_r	T [K]	ζ [V]	E_z [kV m^{-1}]	L [m]
2/3	10^{-6}	80	293	0.2	100	0.01

using FlexPDE. This package is devoted to the solution of systems of partial differential equations through a Rayleigh–Ritz–Galerkin Finite Element Method. The numerical procedure implies an iterative refinement of the grid until the prescribed accuracy, which is related to the maximum local residual value R_k, is reached. The iterative procedure is stopped when the velocity field u^* satisfies the following condition:

$$\max\big(R_k(u^*, N)\big) < \varepsilon \quad \forall k \in [1, N] \tag{10}$$

where N denotes the number of triangular elements. The accuracy of the numerical solution is sensitive to the maximum value of the local residuals, ε, which calls for a sensitivity analysis. By using the same value of ε (10^{-3}) for all the cross sections considered, the required number of triangular elements (N) in order to satisfy the residual-based adaptive refinement criterion, ranges between a minimum value of 80 000 and a maximum value of 150 000. The choice of the value of ε corresponds to a relative value of the residuals lower than 0.1%. The results for DIUF water flowing in a microchannel with a rectangular cross-section were compared with those presented by Arulanandam and Li [11] under the same operating conditions, which are reported in Table 2.

The volume flow rate calculated as a function of the hydraulic diameter is plotted in Fig. 2 for both the rectangular and the trapezoidal cross-sections. The results agree reasonably well with [11], although they overestimate them slightly, showing a maximum difference of about 10% for the largest value of the electro-osmotic diameters considered.

For both cross-sectional areas, the volumetric flow rate is roughly proportional to the second power of the hydraulic diameter and the trapezoidal section allows higher flow rates than the rectangular one for a fixed value of D_h. The increase in Q_v remains approximately constant over the whole range of hydraulic diameters considered. This is also demonstrated in the plot of Fig. 3, which shows the dependence of the equivalent pressure head on the volume flow rate for a rectangular and a trapezoidal cross-section at different values of the electric field driving the fluid. The equivalent pressure head increases linearly with E_z, and the trapezoidal geometry is the more

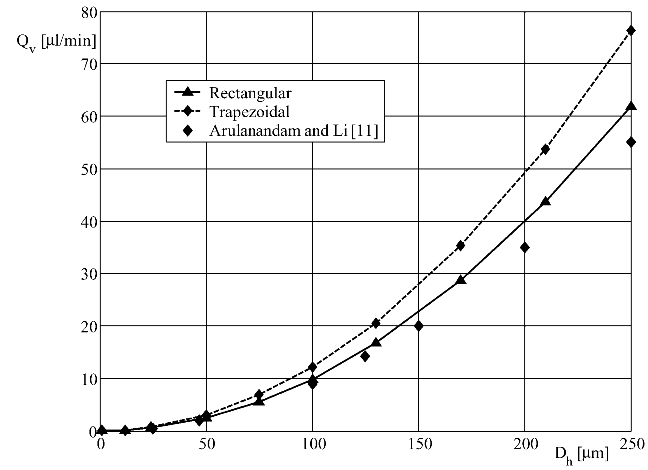

Fig. 2. Volume flow rate as a function of the hydraulic diameter for a rectangular and trapezoidal cross-section and comparison with the results of Arulanandam and Li [11].

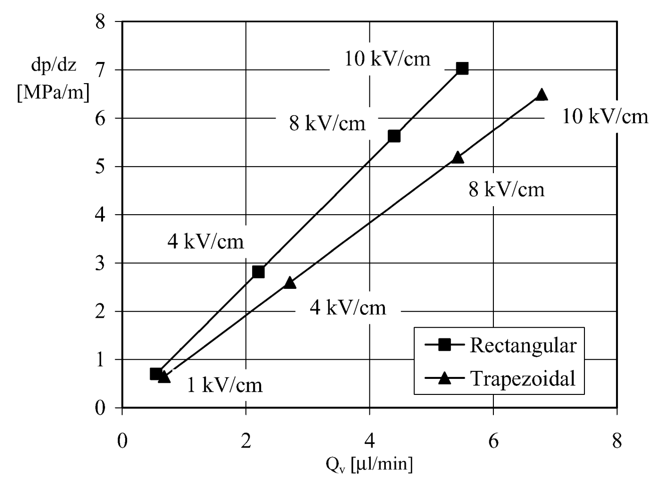

Fig. 3. Equivalent pressure head as a function of the volumetric flow rate for rectangular and trapezoidal cross-section, $\beta = 2/3$ ($\zeta = 0.2$ V, $D_h = 24$ µm, $n_0 = 10^{-6}$ M.)

favourable of the two, as it requires a lower value of the electric potential to be applied at the electrodes for a given flow rate to be circulated in the microchannel. The influence of the aspect ratio is shown in Fig. 4 for a trapezoidal cross section. The triangles refer to a degenerate trapezoidal (i.e. a triangular) cross-section, $\beta = 0.707$, whereas the diamonds are for $\beta = 0.2$. It is clear how lower aspect ratios increase the electroosmotic flow rate.

The data plotted in Figs. 3 and 4 can be useful to calculate the maximum heat flux that can be evacuated by means of a micro heat sink with an electrokinetically-driven flow. Let us consider a heat sink 1 cm × 1 cm in size with 200 microchannels having a hydraulic diameter equal to 24 µm and an aspect ratio β equal to 2/3 (20 µm × 30 µm). DIUF water ($n_0 = 10^{-6}$ M) is considered as working fluid. For a maximum value of the water temperature difference between the inlet and the outlet of the heat sink equal to 50 °C (ΔT) it is possible to calculate the maximum value of the thermal power that can be removed by

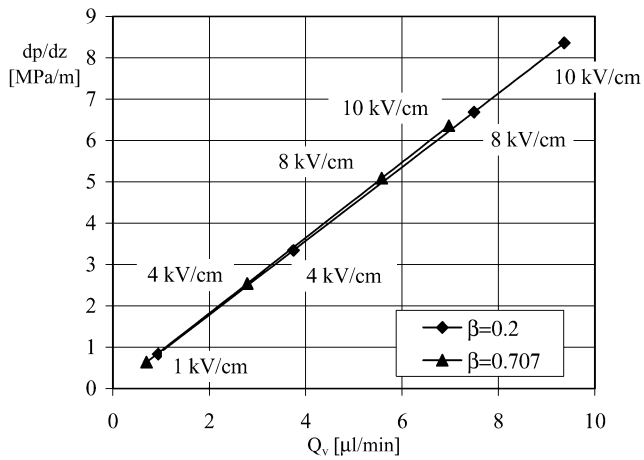

Fig. 4. Equivalent pressure head as a function of the volumetric flow rate for a microchannel of triangular ($\beta = 0.707$) and trapezoidal ($\beta = 0.2$) cross section ($\zeta = 0.2$ V, $D_h = 24$ μm, $n_0 = 10^{-6}$ M).

the heat sink for different values of the electrical potential gradient ($Q_{\rm th} = \rho Q_v c_p \Delta T$).

By using the data plotted in Fig. 3 the value of the volumetric flow rate can be calculated and the maximum removable heat flux can be roughly estimated: the Reynolds number is less than 6 and the maximum heat flux is less than 10 W cm^{-2} for $E_z < 10$ kV cm^{-1}. These results confirm that EOFs can be useful when the hydraulic diameter of the microchannels is less than 50 μm but only low values of volumetric flow rate (low Reynolds numbers) can be obtained.

3. Thermal analysis

In order to calculate the temperature distribution in the microchannel when an electro-osmotic flow is considered under a uniform heat flux at the walls, the energy equation has to be used. In this work fully developed, steady laminar flow conditions are assumed; furthermore, the thermophysical properties are considered independent of the temperature and the effect of viscous dissipation is neglected. In this manner, the Navier–Stokes equations and the energy equation can be considered uncoupled. Under the above-mentioned assumptions, the temperature can be calculated by solving the energy equation written in dimensionless form [8,9]

$$\frac{u^* U}{U_m}\left[\frac{1}{S^*} + M_z\right] = \nabla^{2*} T^* + M_z \tag{11}$$

The dimensionless group:

$$M_z = \frac{E_z^2 \lambda_0 D_h^2}{q'} \tag{12}$$

represents the ratio of Joule heating within the fluid to the heat flux to be removed by forced convection. The boundary conditions to be associated to Eq. (11) are those of uniform heat flux per unit length and uniform temperature along the perimeter of the cross-section:

$$T^*\big|_{C^*} = 0 \tag{13}$$

The average Nusselt number for the cross-section can be determined from the knowledge of the temperature distribution,

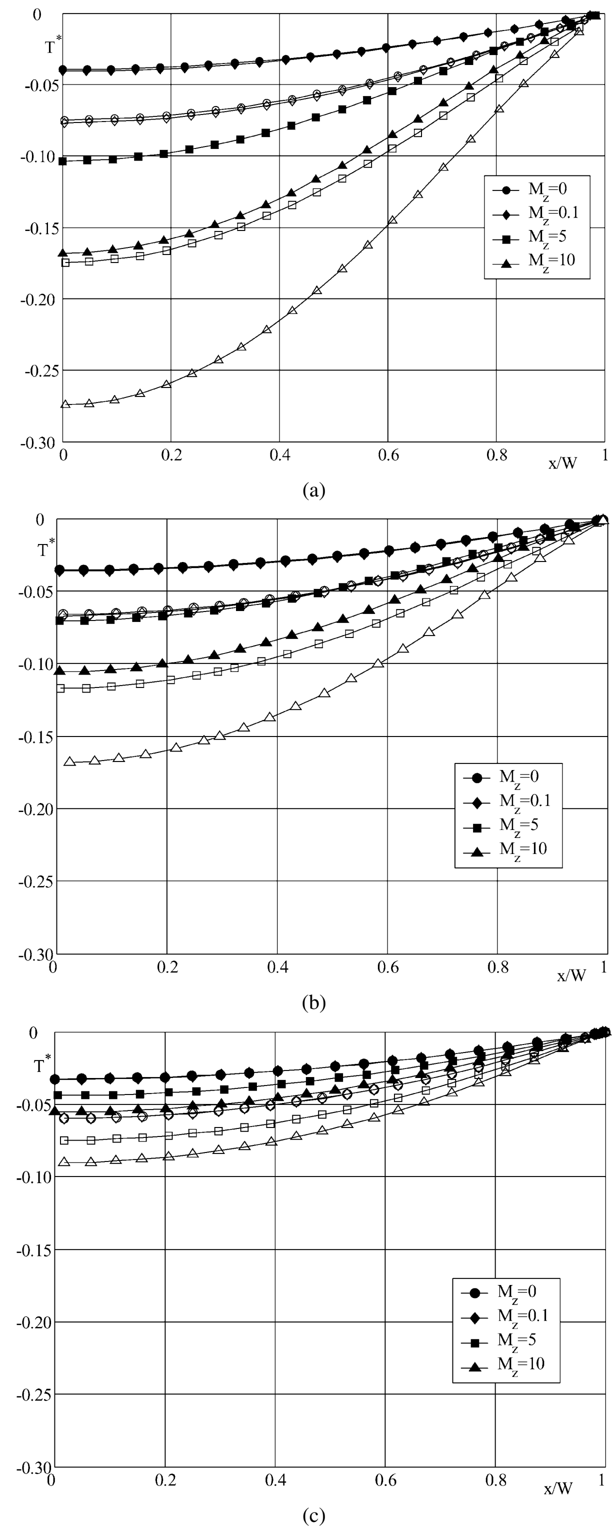

Fig. 5. Temperature profile within rectangular microchannels with an aspect ratio $\beta = 0.25$ (full symbols) and $\beta = 0.50$ (empty symbols): (a) $kD_h = 1$, (b) $kD_h = 10$, (c) $kD_h = 45$.

once the velocity profile is known. The Nusselt number is then obtained from:

$$Nu = -\frac{1}{L^*}\frac{\int_{S^*} u^* \,\mathrm{d}S^*}{\int_{S^*} T^* u^* \,\mathrm{d}S^*} \tag{14}$$

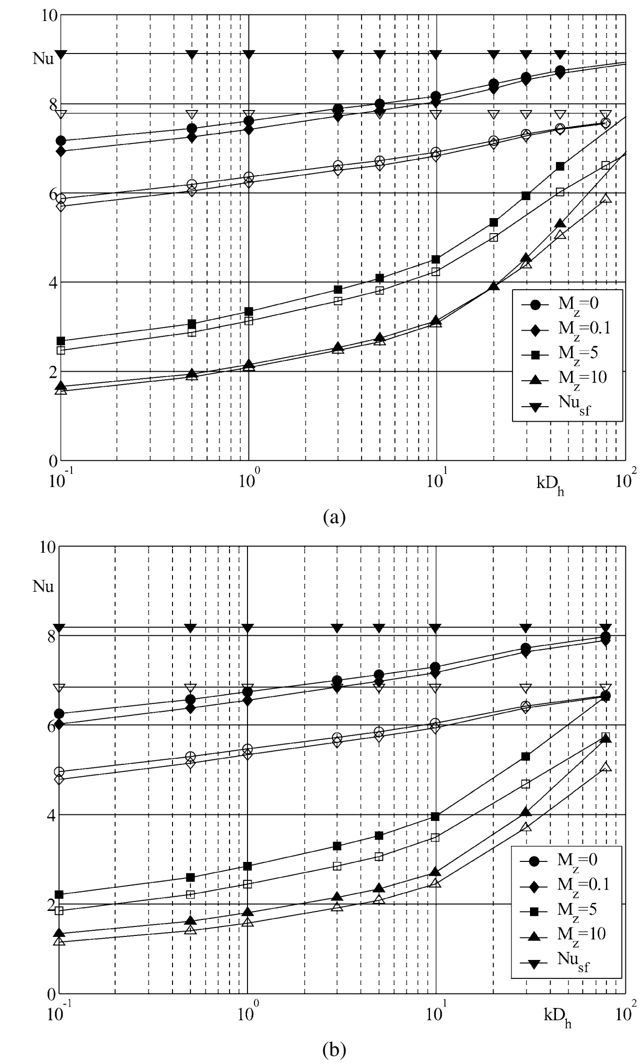

Fig. 6. Nusselt numbers as a function of the electro-osmotic diameter (kD_h) for rectangular (a) and trapezoidal (b) microchannels with an aspect ratio $\beta = 0.25$ (full symbols) and $\beta = 0.50$ (empty symbols). The superscript sf stands for "slug flow".

The temperature profile on the mid-plane ($y/H = 0$) of a rectangular microchannel along its half-width is plotted for three different values of kD_h ($kD_h = 1$, $kD_h = 10$, $kD_h = 45$) in Figs. 5(a), 5(b) and 5(c) respectively. In each figure two different values of the aspect ratio ($\beta = 0.25$, full symbols, and $\beta = 0.50$, empty symbols) are considered, as are four different values of M_z, from no Joule heating to $M_z = 10$. The values of M_z considered in Fig. 5 cover the range of M_z investigated by Maynes and Webb [8,9]. It is evident how the effect of Joule heating decreases when the electrokinetic diameter (kD_h) increases. When the ion concentration increases ($kD_h \to 0$), the influence of Joule heating lowers the non-dimensional temperature remarkably, especially for high values of M_z. This trend becomes more pronounced as the aspect ratio increases. These results confirm the trends evidenced by Maynes and Webb [8,9] for circular microtubes and for parallel plates.

In Fig. 6 the Nusselt number is plotted as a function of kD_h for a microchannel with rectangular (Fig. 6(a)) and trapezoidal (Fig. 6(b)) cross-section for the same values of M_z.

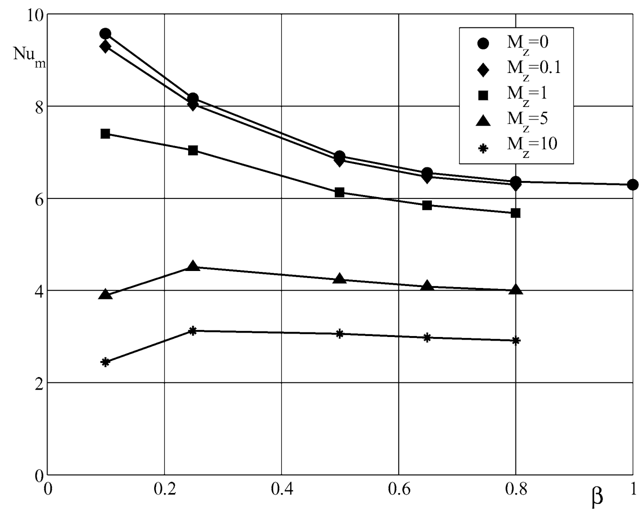

Fig. 7. Nusselt numbers as a function of the aspect ratio for different values of M_z.

It can be noticed how the presence of Joule heating reduces the value of the Nusselt number dramatically, while an increase in the value of the aspect ratio dampens this effect, which is slightly more pronounced in the case of trapezoidal cross-sections. The value of the Nusselt number for a perfectly flat velocity profile (slug flow) as calculated by Morini [14] for rectangular ducts, Nu_{sf}, is also plotted in Fig. 6 for both the rectangular and the trapezoidal cross sections. The values of Nu_{sf} increase as the aspect ratio decreases and they are higher for the rectangular cross section. The values of the Nusselt number approach the corresponding Nu_{sf} when kD_h increases, so much more so the lower the value of M_z.

By observing Figs. 5 and 6, it becomes evident that the effects of the Joule heating can be neglected if M_z is less than 0.1.

Finally, the values of the Nusselt number for a rectangular cross-section as a function of the aspect ratio are plotted in Fig. 7 for $kD_h = 10$ and values of M_z ranging from 0 to 10. It is to be remarked that, while when no Joule heating is considered the highest values of Nu is reached for the parallel plates configuration ($\beta \to 0$), when Joule heating and the wall heat flux become comparable ($M_z = 1$), the Nusselt number presents a maximum for a value of β different from zero, which becomes higher as M_z increases.

4. Conclusions

The thermal-hydraulic characteristics of a microchannel heat sink through which a steady electro-osmotic flow EOF of a polar liquid is circulated were studied numerically. By solving the Poisson–Boltzmann equation and the Navier–Stokes equations, the volumetric flow rate was determined as a function of the hydraulic diameter and of the electrical potential difference applied at the electrodes.

The volumetric flow rate was determined for both trapezoidal and rectangular cross-sections and the former was found to perform better for a fixed value of the electrical potential applied. The influence of the aspect ratio was then investigated and it was proven that lower aspect ratios are to be preferred for the trapezoidal configuration. It has been observed that volumetric flow rates achievable by means of this technique are in general low (low Reynolds numbers). For this reason, the maximum value of the thermal power that can be removed with a micro heat sink with electrokinetically-driven flow ($Q_{\mathrm{th}} = \rho Q_v c_p \Delta T$) is of the order of 10 $\mathrm{W\,cm^{-2}}$ when $E_z < 10\ \mathrm{kV\,cm^{-1}}$.

The thermal problem was then studied, taking the effects of Joule heating within the fluid into account. The non-dimensional temperature profile was obtained for a rectangular cross-section at different values of M_z, kD_h and β. The influence of M_z on the Nusselt number was analysed and it was demonstrated that the values of *Nu* approach that corresponding to slug flow for high values of the electro-osmotic diameter. The results presented in this paper demonstrate that when M_z assumes values less than 0.1 the effects of Joule heating can be considered negligible.

In the future, this analysis will be improved by removing two limitations of the present work: (i) by taking into account the effects related to the variation of the fluid thermophysical properties with temperature, (ii) by considering the effects of the conjugate heat transfer between walls and fluid.

As demonstrated in this work, the Reynolds numbers are in general low for EOF. For this reason, in the analysis of the heat transfer, the contribution related to the axial conduction along the silicon wafer can be important because it changes the axial distribution of the heat flux. A numerical 3D thermal analysis seems to be the best approach to study the heat transfer in the micro heat-sinks with EOFs.

Acknowledgements

This work has been funded through the Italian National Project COFIN 03 by MIUR-URST.

References

[1] F.F. Reuss, Memoires de la Societé Imperiale des Naturalistes de Moskou, vol. 2, 1809, p. 327.

[2] G.M. Mala, D. Li, J.D. Dale, Heat transfer and fluid flow in microchannels, Int. J. Heat Mass Transfer 40 (1997) 3079–3088.

[3] G.M. Mala, D. Li, C. Werner, H.J. Jacobasch, Y.B. Ning, Flow characteristics of water through a microchannel between two parallel plates with electrokinetic effects, Int. J. Heat Fluid Flow 18 (1997) 489–496.

[4] C. Yang, D. Li, Analysis of electrokinetic effects on the liquid flow in rectangular microchannels, Coll. Surface A 143 (1998) 339–353.

[5] C. Yang, D. Li, J.H. Masliyah, Modeling forced liquid convection in rectangular microchannels with electrokinetic effects, Int. J. Heat Mass Transfer 41 (1998) 4229–4249.

[6] D. Li, Electro-viscous effects on pressure-driven liquid flow in microchannels, Coll. Surface A 195 (2001) 35–57.

[7] J.G. Santiago, Electroosmotic flows in microchannels with finite inertial and pressure forces, Anal. Chem. 73 (2001) 2353–2365.

[8] D. Maynes, B.W. Webb, Fully developed electro-osmotic heat transfer in microchannels, Int. J. Heat Mass Transfer 46 (2003) 1359–1369.

[9] D. Maynes, B.W. Webb, Fully-developed thermal transport in combined pressure and electro-osmotically driven flow in microchannels, ASME J. Heat Transfer 125 (2003) 889–895.

[10] G.Y. Tang, C. Yang, J.C. Chai, H.Q. Gong, Joule heating effect on electroosmotic flow and mass transport in a microcapillary, Int. J. Heat Mass Transfer 47 (2004) 215–227.

[11] S. Arulanandam, D. Li, Liquid transport in rectangular microchannels by electroosmotic pumping, Coll. Surface A 161 (2000) 89–102.

[12] G.L. Morini, Laminar liquid flow through silicon microchannels, ASME J. Fluids Engrg. 126 (2004) 485–489.

[13] R.K. Shah, A.L. London, Laminar flow forced convection in ducts, Adv. Heat Transfer 14 (1978) 196.

[14] G.L. Morini, Thermal characteristics of slug flow in rectangular ducts, Int. J. Therm. Sci. 38 (1999) 148–159.